Available online at www.sciencedirect.com
ScienceDirect
Solid State Ionics 179 (2008) 57–60
SOLID STATE IONICS
www.elsevier.com/locate/ssi

# Oxygen nonstoichiometry and ionic transport in $La_2Ni(Fe)O_{4+\delta}$

E.V. Tsipis [a,b], E.N. Naumovich [a], A.L. Shaula [a], M.V. Patrakeev [c], J.C. Waerenborgh [b], V.V. Kharton [a,*]

[a] Department of Ceramics and Glass Engineering, CICECO, University of Aveiro, 3810-193 Aveiro, Portugal
[b] Chemistry Department, ITN/CFMC-UL, Estrada Nacional 10, P-2686-953 Sacavém, Portugal
[c] Institute of Solid State Chemistry, UB RAS, 91 Pervomaiskaya Str., 620219 Ekaterinburg, Russia

**Abstract**

The steady-state oxygen permeation fluxes through dense $La_2NiO_{4+\delta}$ and $La_2Ni_{0.9}Fe_{0.1}O_{4+\delta}$ ceramics, studied at 973–1223 K for membrane thickness range 0.6 to 2.0 mm, are limited by both bulk ambipolar conductivity and surface exchange kinetics. The permeability data, in combination with total conductivity and equilibrium $p(O_2)$–T–$\delta$ diagrams, were used in numerical regression analysis to extract the local chemical potential gradients, defect concentrations, partial conductivities and exchange rates. Doping with iron was found to increase oxygen-ion mobility in $K_2NiF_4$-type lanthanum nickelate at 1173–1223 K, whilst activation energies remain essentially similar, 69–80 kJ/mol. At lower temperatures, the surface kinetics and ionic transport in $La_2Ni_{0.9}Fe_{0.1}O_{4+\delta}$ become both slower than those in $La_2NiO_{4+\delta}$. Possible defect-interaction and exchange mechanisms relevant to this behavior are briefly discussed.


*Keywords:* Lanthanum nickelate; Oxygen permeability; Ionic conductivity; Surface exchange kinetics; Oxygen hyperstoichiometry

## 1. Introduction

Due to high mixed ionic-electronic conductivity and moderate thermal and chemical expansion, the $K_2NiF_4$-type oxide materials derived from oxygen-hyperstoichiometric $La_2NiO_{4+\delta}$ are of significant interest for high-temperature electrochemical applications, such as oxygen separation membranes and cathodes of solid oxide fuel cells [1–7]. The thermal expansion coefficients of these materials vary in the range $(13–15)\times10^{-6}$ $K^{-1}$, whereas the isothermal chemical expansion caused by the oxygen nonstoichiometry variations under oxidizing conditions is lower than 0.05% relative to atmospheric oxygen pressure, providing a good thermomechnical stability compared to the perovskite-type analogues. The ionic transport in $La_2NiO_4$-based phases occurs predominantly via an interstitial migration mechanism; the incorporation of extra oxygen into rock-salt LaO bilayers of the $K_2NiF_4$-type structure is charge-compensated by hole generation in the perovskite sheets formed by $NiO_6$ octahedra [1,2,7]. The oxygen permeation through dense nickelate membranes is limited by both surface exchange kinetics and bulk ambipolar conduction [4,6]. Doping with higher-valence cations, such as iron, leads to a higher hyperstoichiometry [4,7], which may have positive effects on the ionic transport. The present work focuses on modelling of the oxygen permeation processes in $La_2NiO_{4+\delta}$ and $La_2Ni_{0.9}Fe_{0.1}O_{4+\delta}$ membranes. The data on oxygen nonstoichiometry, used for the analysis of ionic conduction and surface exchange, and the models describing defect formation in $La_2NiO_4$-based compounds were reported in previous works [7,8].

## 2. Theory

The equilibrium $p(O_2)$–T–$\delta$ diagrams of $La_2Ni(Fe)O_{4+\delta}$ can be adequately described by a statistical-thermodynamic approach, introducing point-defect interaction energy in the concentration-dependent part of defect chemical potentials and accounting for the site-exclusion effects [7,8]. The critical factors include coulombic repulsion, trapping of the p-type

* Corresponding author. Tel.: +351 234 370263; fax: +351 234 425300.
*E-mail address:* kharton@ua.pt (V.V. Kharton).

0167-2738/$ - see front matter © 2007 Elsevier B.V. All rights reserved.
doi:10.1016/j.ssi.2007.12.026

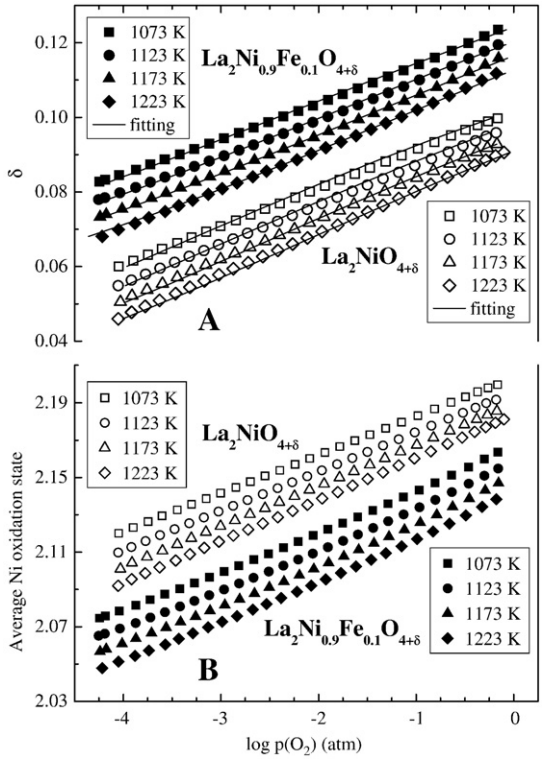


Fig. 1. Oxygen partial pressure dependencies of the oxygen nonstoichiometry (A) and average oxidation state of nickel cations (B) in $La_2Ni_{0.9}Fe_{0.1}O_{4+\delta}$ in comparison with $La_2NiO_{4+\delta}$. Solid lines correspond to the fitting results.

electronic charge carriers by donor-type cations such as iron, and interaction between these cations and electron holes. Briefly, these effects can be expressed by the discrete Fermi-Dirac distribution and the general equation for the defect chemical potential ($\mu$):

$$\mu\left(\mathrm{Df}_x^z\right) = \mu^0\left(\mathrm{Df}_x^z\right) + \mathrm{RT}\cdot\ln a\left(\mathrm{Df}_x^z\right) = \mu^0\left(\mathrm{Df}_x^z\right) + \mathrm{RT}\cdot\ln\frac{\left[\mathrm{Df}_x^z\right]}{N\left(\mathrm{Df}_x^z\right) - \left[\mathrm{Df}_x^z\right]} \quad (1)$$

where $[Df_X^z]$ is the concentration of defects $Df_X^z$ in the $X$ sublattice, $z$ is their charge, $N(Df_X^z)$ is the number of states, and $a$ is the activity. The discrete density of states is to be assessed statistically, by analyzing the probability of different defect configurations for a fixed overall composition via the binomial distribution:

$$P\left(Df_x^z, Nh_Y^w, m\right) = \binom{n_{YX}}{m} \times \left(\frac{\left[Nh_Y^w\right]}{\left[Y_{\max}\right]}\right)^m \left(1 - \frac{\left[Nh_Y^w\right]}{\left[Y_{\max}\right]}\right)^{n_{YX}-m} \quad (2)$$

where $Nh_Y^w$ is a lattice element introduced in the same or another sublattice ($Y$) and affecting $\mu(Df_X^z)$, $n_{YX}$ is the number of $Y$ sites neighboring the given $X$ position, $w$ is the charge of $Nh_Y^w$ species, $m$ is their number in the $X$ neighborhood, $\binom{n_{YX}}{m}$ is the binomial coefficient, and $[Y_{max}]$ is the number of $Y$ sites per formula unit.

The p-type electronic charge carriers in $La_2NiO_{4+\delta}$, located on nickel cations, were assumed to exclude the presence of other holes in the nearest neighborhood; a similar effect was considered for interstitial $O^{2-}$ anions [7]. In the case of $La_2Ni_{0.9}Fe_{0.1}O_{4+\delta}$, most iron cations were found to be trivalent, in equilibrium with mobile holes and $Fe^{2+}$ and to partly block nearest-neighboring sites for the p-type carriers [8]. The dominant 3+ oxidation state of iron was confirmed by Mössbauer spectroscopy [8]. These hypotheses made it possible to adequately describe the equilibrium $p(O_2)$–T–$\delta$ diagrams of $La_2Ni_{0.9}Fe_{0.1}O_{4+\delta}$ and $La_2NiO_{4+\delta}$, as illustrated by Fig. 1.

The oxygen permeation fluxes ($j$) through dense $La_2Ni(Fe)O_{4+\delta}$ ceramics were modeled splitting the overall oxygen chemical potential gradient into three parts, corresponding to the membrane bulk ($\Delta\mu^{bulk}$), the permeate-side ($\Delta\mu_1^{surf}$) and the feed-side ($\Delta\mu_2^{surf}$) surfaces, Fig. 2. The former contribution is determined by the partial ionic ($\sigma_o$) and electronic ($\sigma_e$) conductivities according to the Wagner law:

$$j = \frac{1}{16F^2L}\int_{\mu_1^{surf}}^{\mu_2^{surf}} \frac{\sigma_o\sigma_e}{\sigma_o+\sigma_e} d\mu(O_2) = \frac{\mathrm{RT}}{16F^2L}\int_{\ln p_1^s}^{\ln p_2^s} \sigma_o\left(1-\frac{\sigma_o}{\sigma}\right) d\ln p(O_2) \quad (3)$$

where $L$ is the membrane thickness, $\sigma$ is the total conductivity measured experimentally as function of the oxygen partial pressure, $p_1^s$ and $p_2^s$ are the $p(O_2)$ values at the permeate- and feed-side surfaces, respectively. The ionic conductivity was defined by the classical model (e.g., [9]):

$$\sigma_o = 2eu_o\left[O_i^{2-}\right]Z_{fu}/V_{uc} \quad (4)$$

where $[O_i^{2-}]$ is the concentration of oxygen interstitials per unit formula, $u_o$ is the anion mobility, $Z_{fu}=2$ is the number of formula units per unit cell (space group *I4/mmm*), and $V_{uc}$ is

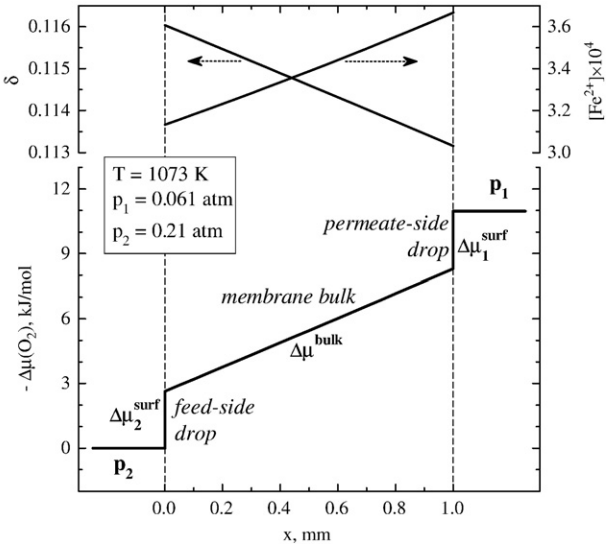


Fig. 2. Example of the calculated distributions of hyperstoichiometric oxygen content, concentration of divalent iron cations, and oxygen chemical potential increment relative to atmospheric air supplied onto the membrane feed-side surface, for one $La_2Ni_{0.9}Fe_{0.1}O_{4+\delta}$ membrane with $L=1.00$ mm. External conditions are given in the legend.

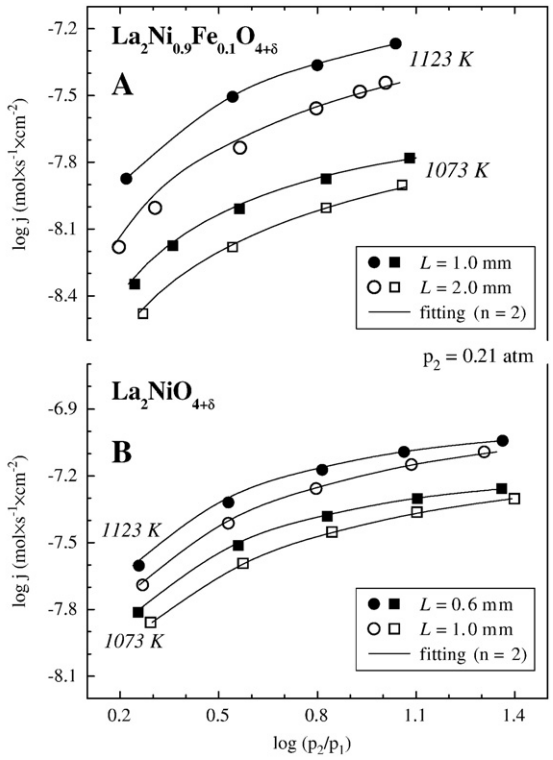


Fig. 3. Oxygen permeation fluxes through dense $La_2NiO_4$-based membranes with different thicknesses vs. oxygen partial pressure gradient. Solid lines correspond to the fitting results.

the unit cell volume calculated from the structural data. The oxygen transfer through membrane/gas interface was simulated as

$$j = J^0 \cdot \left(1 - \exp\left[\frac{\Delta\mu_i^{surf}}{nRT}\right]\right) \quad (5)$$

where $J^0$ and $n$ are constants. Eq. (5) is, again, a classical non-equilibrium thermodynamic expression [10], with $J^0$ corresponding to the equilibrium exchange rate and $n$ being the stoichiometric coefficient which shows the relationship between the fluxes of molecular $O_2$ and species involved in the rate-determining step. This formula represents a simplified solution of the model proposed for oxygen exchange between a mixed conductor and gas phase [11], and is also qualitatively similar to the equation describing solid-electrolyte cells where increasing electrode polarization leads to limiting currents [12,13]. In the latter case, physical meaning of $J^0$ relates to the limiting flux of electrochemically active species, which may be governed by diffusion, adsorption or chemical reaction steps [12,13]. Eq. (5) was selected from more than 10 alternative models, including the Butler-Volmer type formulae and various kinetic and thermodynamic equations [10–13], on the basis of fitting results. In the course of regression analysis of the oxygen permeation data, this set of equations was solved numerically with $j$, $\mu_2$ and $L$ as independent variables; the relationships between $[O_i^{2-}]$ and oxygen chemical potential were described using the fitting parameters for equilibrium $p(O_2)$–T–$\delta$ diagrams (Fig. 1).

## 3. Experimental

Submicron powders of $La_2NiO_{4+\delta}$ and $La_2Ni_{0.9}Fe_{0.1}O_{4+\delta}$ were prepared by the glycine-nitrate process [14]. After synthesis, the powders were annealed in air at 1073–1373 K for 2–5 h, ball-milled and then pressed into disks at 150–250 MPa. Gas-tight ceramics with 95–98% density were sintered in air at 1593–1723 K during 2–10 h and cooled down to room temperature at 1–2 K/min to achieve equilibrium with atmospheric oxygen. The powdered samples used for X-ray diffraction (XRD), coulometric titration (CT), thermogravimetric analysis (TGA) and Mössbauer spectroscopy, were obtained by grinding of dense ceramics. For Mössbauer spectroscopy studies, the ceramics was prepared under identical conditions, but using $^{57}Fe$ isotope-enriched metallic iron as one of starting materials; analysis of the Mössbauer spectra is found in Ref.[8]. Formation of single $K_2NiF_4$-type phases and their cation composition were verified by XRD, inductively-coupled plasma and energy dispersive spectroscopic analyses. The experimental techniques used to determine absolute oxygen content (CT and TGA), total electrical conductivity (4-probe DC) and steady-state oxygen permeation fluxes are described elsewhere [6–8,15,16]. For all permeation data presented in this work, the feed-side oxygen partial pressure ($p_2$) was fixed at 0.21 atm.

## 4. Results and discussion

Fig. 3 presents selected oxygen permeation data for $La_2Ni(Fe)O_{4+\delta}$ membranes with different thickness; the fitting results are shown by solid lines. The best fitting quality was obtained fixing $n$=2. While introducing $n$ as a regression parameter caused statistical degeneration, the use of other possible values, such as 4 or 1, resulted in significantly higher error. This suggests that the rate-determining step of oxygen surface exchange may involve species related to one oxygen atom or site participating in the reaction. The tendency to limiting fluxes may appear due to stagnated surface migration of such species or

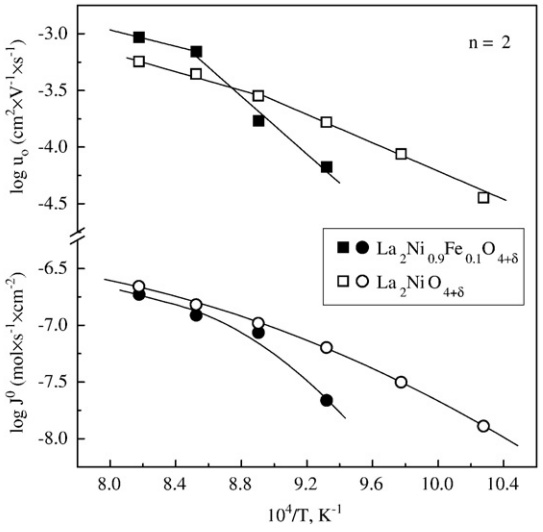


Fig. 4. Temperature dependencies of the oxygen ion mobility and surface exchange rates of $La_2Ni_{0.9}Fe_{0.1}O_{4+\delta}$ and $La_2NiO_{4+\delta}$ ceramics.

slow vacancy formation/diffusion from the membrane bulk. The discharge of intermediate ionic species, intercalated in or deintercalated from the lattice, should be fast since the electronic conductivity of $La_2NiO_4$-based phases is much higher than ionic [1–7]; as the content of hyperstoichiometric oxygen is low with respect to the concentration of interstitial positions, the latter factor cannot be critical as well. Whatever the exact mechanisms, the estimated oxygen chemical potential drop at the feed-side surface is almost equal to that at the permeate-side (Fig. 2), probably indicating a similar nature of rate-limiting steps. Moreover, attempts to introduce different exchange currents for oxygen reduction and evolution processes failed. Notice also that essentially linear distributions of the oxygen-interstitial and $Fe^{2+}$ concentrations across the membrane correlate with linearity of the equilibrium $\delta$ vs. ln $p(O_2)$ dependencies (Figs. 1 and 2), caused by strong point-defect interactions [7,8].

Another important tendency relates to decreasing activation energies for the ion mobility and surface exchange when temperature increases up to 1120–1170 K (Fig. 4). Analogous trends are well known for other perovskite-related mixed conductors, including $La_2Ni(Co)O_{4+\delta}$ and $(La,Sr)(Fe,Ga)O_{3-\delta}$, and for various solid-electrolyte materials [6,15,17]. In the latter cases, such behavior originates from progressive disordering in the oxygen sublattice on heating. For $La_2Ni(Fe)O_{4+\delta}$ and $La_2Ni(Co)O_{4+\delta}$, the electron diffraction studies showed no evidence of ordered microdomains or superlattices [6,8], although the long-range ordering phenomena at low temperatures can still be expected. The variations in the ion mobility activation energy at 1170 K are hence ascribed to other factors, primarily to decreasing coulombic repulsion forces between the oxygen interstitials due to thermal expansion. The coulombic interaction between $O^{2-}$ anions in the rock-salt type layers of $K_2NiF_4$-type structure has a substantial effect on the oxygen thermodynamics [7,8] and may also hamper interstitial migration in $La_2NiO_4$-based compounds. Consequently, at temperatures below 1150 K a higher anion mobility is observed for undoped lanthanum nickelate where the oxygen excess is lower than that in $La_2Ni_{0.9}Fe_{0.1}O_{4+\delta}$ (Fig. 1). The corresponding activation energies are 125 and 244 kJ/mol, respectively. Reducing $\delta$ on heating increases the concentration of available interstitial positions, thus increasing the role of the ion-jump stereological parameters, primarily the radius of migration channels (so-called “bottleneck radius”). These parameters are, again, stoichiometry-dependent. In particular, oxygen intercalation leads to the tetragonal unit cell expansion along the *c* axis [5,8] and, therefore, enlarges the interstitial–diffusion channel size. As a result, the anion mobility in $La_2Ni_{0.9}Fe_{0.1}O_{4+\delta}$ achieves higher values compared to $La_2NiO_{4+\delta}$ at 1173–1223 K (Fig. 4); the activation energies become close to each other, 69–80 kJ/mol. The behavior of surface exchange kinetics follows qualitatively similar trends, confirming a key role of oxygen vacancies formed in the perovskite-like layers due to intrinsic Frenkel disordering. Since the vacancy concentration is reciprocal function of the extra oxygen content, undoped $La_2NiO_{4+\delta}$ exhibits a faster exchange with respect to the Fe-containing material.

In summary, the results show that the substitution of iron for nickel increases both concentration and mobility of oxygen interstitials in $La_2Ni(Fe)O_{4+\delta}$ lattice at temperatures above 1150 K. This advantageous effect, in combination with appropriate surface-modification methods, makes it possible to improve performance of nickelate-based membranes in the high-temperature range. The deposition of catalytically-active layers and/or increasing membrane surface area is necessary to enhance interfacial exchange rates, which limit oxygen permeation and decrease on doping.

## Acknowledgements

This work was supported by FCT, Portugal (projects POCI/CTM/59197/2004, PTDC/CTM/64357/2006, SFRH/BPD/28629/2006 and SFRH/BPD/28913/2006).

## References

[1] G. Amow, S.J. Skinner, J. Solid State Electrochem. 10 (2006) 538.
[2] F. Mauvy, C. Lalanne, J.-M. Bassat, J.-C. Grenier, H. Zhao, L. Huo, Ph. Stevens, J. Electrochem. Soc. 153 (2006) A1547.
[3] V.V. Vashook, I.I. Yushkevich, L.V. Kokhanovsky, L.V. Makhnach, S.P. Tolochko, I.F. Kononyuk, H. Ullmann, H. Altenburg, Solid State Ionics 119 (1999) 23.
[4] B. Vigeland, R. Glenne, T. Breivik, S. Julsrud, Int. Patent Application PCT WO 99/59702 (1999).
[5] V.V. Kharton, A.V. Kovalevsky, M. Avdeev, E.V. Tsipis, M.V. Patrakeev, A.A. Yaremchenko, E.N. Naumovich, J.R. Frade, Chem. Mater. 19 (2007) 2027.
[6] V.V. Kharton, A.A. Yaremchenko, E.V. Tsipis, A.A. Valente, M.V. Patrakeev, A.L. Shaula, J.R. Frade, J. Rocha, Appl. Catal., A 261 (2004) 25.
[7] E.N. Naumovich, M.V. Patrakeev, V.V. Kharton, A.A. Yaremchenko, D.I. Logvinovich, F.M.B. Marques, Solid State Sci. 7 (2005) 1353.
[8] E.V. Tsipis, E.N. Naumovich, M.V. Patrakeev, J.C. Waerenborgh, V. Ye, P. Pivak, P. Gaczyński, V.V. Kharton, J. Phys. Chem. Solids. 68 (2007) 1443.
[9] P. Kofstad, Nonstoichiometry, Diffusion and Electrical Conductivity in Binary Metal Oxides, Wiley-Interscience, New York, 1972.
[10] S.R. De Groot, P. Mazur, Nonequilibrium Thermodynamics, Dover, New York, 1984.
[11] S.B. Adler, X.Y. Chen, J.R. Wilson, J. Catal. 245 (2007) 91.
[12] Fuel Cell Handbook, EG&G Technical Services, Inc. Science Applications International Corporation, Morgantown, West Virginia, 6th ed., 2002.
[13] V.N. Chebotin, M.V. Perfiliev, Electrochemistry of Solid Electrolytes, Technical Information Center, US Department of Energy, Oak Ridge, 1978.
[14] L.A. Chick, L. Pederson, G.D. Maupin, J.L. Bates, L.E. Thomas, G.L. Exarhos, Mater. Lett. 10 (1990) 6.
[15] V.V. Kharton, A.A. Yaremchenko, A.P. Viskup, M.V. Patrakeev, I.A. Leonidov, V.L. Kozhevnikov, F.M. Figueiredo, A.L. Shaulo, E.N. Naumovich, F.M.B. Marques, J. Electrochem. Soc. 149 (2002) E125.
[16] M.V. Patrakeev, E.B. Mitberg, A.A. Lakhtin, I.A. Leonidov, V.L. Kozhevnikov, V.V. Kharton, M. Avdeev, F.M.B. Marques, J. Solid State Chem. 167 (2002) 203.
[17] V.V. Kharton, F.M.B. Marques, A. Atkinson, Solid State Ionics 174 (2004) 135.